Calculation of Electron Detachment Energies for Water Cluster Anions: An Appraisal of Electronic Structure Methods, with Application to $(H_2O)_{20}^-$ and $(H_2O)_{24}^-$

John M. Herbert* and Martin Head-Gordon

Department of Chemistry, University of California, Berkeley, California 94720

Received: March 3, 2005; In Final Form: April 24, 2005

We present benchmark calculations of vertical electron detachment energies (VDEs) for various conformers of $(H_2O)_n^-$, using both wave function and density functional methods, in sequences of increasingly diffuse Gaussian basis sets. For small clusters ($n \leq 6$), a systematic examination of VDE convergence reveals that it is possible to converge this quantity to within ∼0.01 eV of the complete-basis limit, using a highly diffuse but otherwise economical Pople-style basis set of double-ζ quality, with 28 atom-centered basis functions per water molecule. Floating-center basis functions can be useful but are not required to obtain accurate VDEs. Second-order Møller−Plesset perturbation (MP2) theory suffices to obtain VDEs that are within 0.05 eV of the results from both experiment and coupled-cluster theory, and which always err toward underbinding the extra electron. In contrast to these consistent predictions, VDEs calculated using density functional theory (DFT) vary widely, according to the fraction of Hartree−Fock exchange in a given functional. Common functionals such as BLYP and B3LYP overestimate the VDE by 0.2−0.5 eV, whereas a variant of Becke's "half and half" functional is much closer to coupled-cluster predictions. Exploratory calculations for $(H_2O)_{20}^-$ and $(H_2O)_{24}^-$ cast considerable doubt on earlier calculations that were used to assign the photoelectron spectra of these species to particular cluster isomers.

I. Introduction

Water cluster anions, $(H_2O)_n^-$, have long garnered attention as finite analogues of the aqueous electron.[1−14] The extent to which this analogy is convincing, however, is dependent on the manner in which the "excess" electron is solvated by the cluster, and this remains controversial—or simply unknown—at almost all cluster sizes. For $n > 11$, photodetachment measurements on size-selected clusters[3,4,14] reveal that the vertical electron detachment energy (VDE) of $(H_2O)_n^-$ increases linearly as a function of $n^{-1/3}$, which suggests cavity-like solvation, analogous to the bulk hydrated electron.[15,16] However, theoretical calculations[17−19] predating these photodetachment experiments indicate that the aforementioned VDEs correspond to surface-bound states of the excess electron, whereas internally solvated states are predicted to have significantly larger VDEs than those measured originally.[3,4] Calculated optical absorption spectra[19] for these purported surface states are also in good agreement with experimental results,[5,20] despite the fact that the experimental excitation energies and linewidths both scale linearly with $n^{-1/3}$. On the other hand, these calculations use an electron-water pseudo-potential that is known to overbind the electron,[21] whereas the recent observation of a slew of previously unobserved, weakly bound $(H_2O)_n^-$ isomers, combined with an ad hoc scaling of the calculated VDEs, furnishes a tantalizing coincidence between theory and experiment for both weakly bound and strongly bound isomers.[14]

The photoelectron spectrum alone provides little structural information, whereas, in principle, electronic structure theory provides the means to elucidate the isomeric origins of both peak positions and peak widths in such spectra. Although much has already been written[9,22−44] concerning the electronic structure of $(H_2O)_n^-$, where $n = 2-24$, there has been no systematic characterization of the accuracy of methods such as density functional theory (DFT) and second-order Møller−Plesset (MP2) perturbation theory that are tractable for large clusters ($n > 6$). Similarly, there has been no systematic study of VDE convergence leading to general recommendations regarding basis sets appropriate for $(H_2O)_n^-$. Although previous studies of weakly bound anions have examined the convergence of VDEs with respect to the one-electron basis set,[45,46] these studies intended to achieve ∼1 meV accuracy in VDEs, which requires basis sets that would be impractical for large systems, not only because of their size but also because of the crippling linear dependencies that result when a large number of highly diffuse basis functions (especially those with high angular momentum) is used. For many applications, such accuracy may not be absolutely necessary; various isomers of $(H_2O)_n^-$, for example, can be distinguished at much lower resolution. With this in mind, we set the bar somewhat lower and aim to predict VDEs consistently (i.e, for different isomers and different cluster sizes) to an accuracy of ∼50 meV, with respect to both experiment and higher-level calculations.

In the present study, convergence to the complete-basis limit is assessed systematically using a sequence of increasingly diffuse basis sets. For correlated wave function methods, we find that VDEs are exquisitely sensitive to the diffuseness of the Gaussian basis functions but, within the target accuracy identified previously, are remarkably *insensitive* to other qualities of the basis set. A double-ζ quality basis, containing three diffuse shells and 28 basis functions per water molecule, yields VDEs that are converged to within 10 meV of the complete basis set (CBS) limit at a given level of theory. Notably, we are able to converge the VDE using only atom-centered basis

* Author to whom correspondence should be addressed. Phone: 510-643-4304. Fax: 510-643-1255. E-mail: jherbert@calmail.berkeley.edu.

10.1021/jp051096s CCC: $30.25
Published on Web 05/24/2005

functions, thus providing a "model chemistry" prescription[47] that does not require careful, system-dependent optimization of floating-center basis functions and that treats both localized and delocalized surface-bound electrons on an equal footing.

Although numerical linear dependencies can render VDE calculations computationally laborious, within our target accuracy the $(H_2O)_n^-$ system is not especially challenging with regard to the treatment of electron correlation: MP2 consistently affords VDEs that are ~50 meV below both experiment and coupled-cluster predictions. Error of this magnitude is acceptable, provided that it is not comparable to the VDE itself, and, fortunately, the isomers of $(H_2O)_n^-$ observed in the photoelectron spectra fit this description. Thus, MP2 calculations in relatively small basis sets are sufficient to distinguish between isomers and to provide semiquantitative VDEs. On the other hand, common density functionals such as BLYP[48,49] and B3LYP[50,51] overestimate VDEs by 200−300 meV for small clusters. A slightly more exotic functional that combines Becke's "half and half" exchange[52] with Lee−Yang−Parr (LYP) correlation,[49] which we denote as BHLYP,[53] comes quite close to coupled-cluster VDE predictions.

Thus far, large water cluster anions have been scrutinized theoretically only with B3LYP[40−42] and pseudo-potential methods;[17−19] therefore, as an application of our findings, we examine $(H_2O)_{20}^-$ and $(H_2O)_{24}^-$ at the MP2 level and compare these results to those obtained using various density functionals. Our findings cast serious doubt on VDEs calculated previously for these systems,[40−42] which were used to assign particular isomers to the measured photoelectron spectra.

II. Computational Details

In this work, we report VDEs for anionic clusters,

$$\mathrm{VDE} = E(\text{neutral at optimized anion geometry}) - E(\text{anion})$$

as well as vertical attachment energies (VAEs) for neutral clusters,

$$\mathrm{VAE} = E(\text{anion at optimized neutral geometry}) - E(\text{neutral})$$

A positive VDE indicates that the anion is at least metastable with respect to autodetachment, whereas a negative VAE indicates that spontaneous electron capture is possible at the cluster geometry in question. A negative VDE that has been obtained using finite-basis electronic structure theory is less conclusive. In such cases, one is dealing with a discretized continuum state, because the anion is unstable but is prevented by the finite basis from ejecting the unwanted electron. At a given level of theory, the VDE might be positive in the CBS limit, indicating a (meta)stable anion, or it might tend to zero if the anion is, indeed, unbound.

Wave function-based calculations reported here include Hartree−Fock (HF) theory, MP2 perturbation theory, coupled-cluster[54] singles and doubles (CCSD), and CCSD with noniterative triples [CCSD(T)]. Core orbitals were uncorrelated, as core excitations were determined to contribute <1 meV to VDEs. We also report DFT calculations using the familiar BLYP[48,49] and B3LYP[50,51] functionals, as well as the BHLYP functional[52,53] described previously and the recently developed X3LYP functional,[55−57] which has been shown to perform well for neutral water clusters.[56] All calculations were performed using the Q-CHEM program.[58] Molecular structures and orbital plots were rendered using MOLDEN[59] and Visual Molecular Dynamics.[60]

A common technique to accelerate basis-set convergence in VDE calculations is to use "floating center" or "ghost atom" basis functions whose positions are fixed, by symmetry if not by fiat, or else optimized along with the molecular geometry. However, even optimized floating centers require some basic assumptions regarding their initial placement, and, furthermore, this approach is unlikely to provide a balanced description of surface-bound states versus internalized (cavity) states of the excess electron. Our experience also indicates that the potential energy surface is very flat with respect to the positions of the ghost atoms, leading to protracted geometry optimizations. (Admittedly, this cost is sometimes offset by a reduction in the size or linear dependence of the basis set.) In any case, one major objective of the present study is to confirm[61] that VDEs can be converged to the CBS limit, using only atom-centered basis functions, without introduction of untoward linear dependencies.

In the interest of a systematic study leading to simple basis-set recommendations, we construct basis sets by augmenting standard Dunning- and Pople-style bases with a sequence of increasingly diffuse *s* functions for the H atoms and *sp* functions (even-tempered *s* and *p* functions) for the O atoms. We expect that this is qualitatively sufficient to model the singly occupied molecular orbital (SOMO) in $(H_2O)_n^-$, because this orbital has primarily *s* character, along with a small admixture of *p* character that allows the SOMO to delocalize over several dangling H atoms. The necessary *p* character can result either from *p* orbitals on the O atoms or simply from the mixing of *s* orbitals on nearby H atoms, and we leave it up to the calculations reported in Section III to determine which is quantitatively more important. Diffuse *p* functions on the H atoms were not considered, to limit the size of the basis, while diffuse functions beyond *p* were omitted (except as already present in Dunning's aug-cc-pV*N*Z basis sets), because previous studies of dipole-bound anions suggest that diffuse *d* functions contribute, at the most, a few millielectron volts to the VDE.[45,46,62]

The first set of diffuse functions on any given atom are the standard Pople ("+") or Dunning ("aug") functions, and, thereafter, the orbital exponent for each new shell is reduced from the last by a constant geometric progression factor *p*, which is assumed to be $^1/_3$, unless otherwise noted. Augmented Dunning basis sets constructed in this way are denoted as as aug*M*-cc-pV*N*Z, where *M* indicates the number of diffuse shells and aug1-cc-pV*N*Z ≡ aug-cc-pV*N*Z. Pople-style diffuse basis sets are denoted, for example, as 6-31(*m*+*n*+)G*, meaning *m* sets of diffuse *sp* functions on each oxygen and *n* diffuse *s* functions on each hydrogen. Finally, we define floating-center basis sets 6-31(*m*+*n*+)G*-f(*k*+), which consist of a single ghost atom that is treated as a heavy atom augmented with *k* sets of diffuse *sp* functions.

Extremely diffuse basis functions complicate electronic structure calculations by introducing (near) linear dependencies that lead to a poorly conditioned overlap matrix, thereby necessitating tight thresholds. The calculations reported here use a drop tolerance of 10^{-14} (in atomic units (au), in the case of integral thresholds), while eigenvectors of the overlap matrix corresponding to eigenvalues of $<10^{-7}$ are projected out of the atomic orbital basis. A typical case is $(H_2O)_{24}^-$ in the 6-31(1+3+)G* basis, where projection removes approximately three basis functions out of 672. (The precise number is dependent on geometry.) Most self-consistent field (SCF)

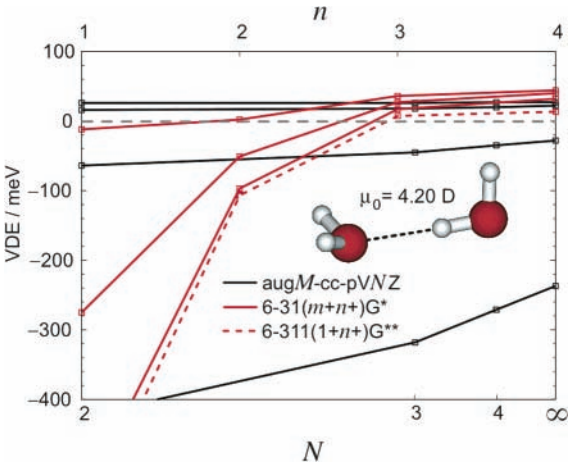

Figure 1. Second-order Møller−Plesset (MP2) detachment energies for *cis*-$(H_2O)_2^-$. *M* and *m* increase from bottom to top across the data sets, and *N* is plotted on an $N^{-1/3}$ scale, reflecting our complete basis set (CBS) extrapolations. The broken gray line indicates VDE = 0.

calculations were converged to a threshold of 10^{-9} au in the occupied-virtual elements of the Fock matrix, typically using geometric direct minimization;[63] however, we found it impossible to converge certain DFT calculations this tightly. (BLYP is especially problematic.) For these troublesome cases, the SCF convergence criterion was relaxed to 10^{-7} or 10^{-8} au.

Numerical integration in DFT calculations uses the "standard grid" SG-1,[64] which is a pruned Euler−Maclaurin−Lebedev grid that consists of 50 radial points and 194 angular points per atom. To verify the accuracy of this grid for extremely diffuse densities, we tested several alternatives on three isomers of $(H_2O)_6^-$ having VDEs in the range of 20−74 meV. For these cases, an *unpruned* grid that consists of 99 radial points[65] and 590 angular points per atom (218 890 total grid points, versus 14 712 points using SG-1) afforded VDEs that differed by <1 meV from those calculated using SG-1, for all of the Pople-style basis sets used in this work. The more sparse SG-0 grid gave larger discrepancies and was rejected. As an additional test, we repeated our aug4-cc-pVQZ calculations for $(H_2O)_2^-$ using an unpruned grid of 99 radial points and 302 angular points per atom. In this case, the BLYP and B3LYP detachment energies differed by <1 meV between the two grids, while the VDE for X3LYP changed by 7 meV. Thus, we deem SG-1 to be adequate.

III. Results and Discussion

A. Water Dimer Anion. Our investigation begins with the water dimer anion, which has a measured VDE of only 45 meV.[3] Previous calculations[29,35] have identified the cis isomer as the species responsible for the photoelectron spectrum, and we optimized the geometry of *cis*-$(H_2O)_2^-$ at the MP2/aug3-cc-pVDZ level to obtain an equilibrium geometry, dipole moment (of the corresponding neutral dimer), and vibrational frequencies very close to those reported in ref 35.

Given its small VDE and concomitantly diffuse electron density, even the ordinarily high-quality aug-cc-pV*N* Z basis sets provide a poor estimate of the VDE in the CBS limit. Figure 1 charts the convergence of MP2 detachment energies using correlation-consistent basis sets, aug*M*-cc-pV*N* Z, with corresponding numerical data presented in Table 1. Points labeled $N = \infty$ in Figure 1 are the result of two-point extrapolations versus $N^{-1/3}$, where the absolute energies of $(H_2O)_2$ and $(H_2O)_2^-$ were extrapolated separately; we denote these extrapolations as CBS-*M*, where *M* implies that the aug*M*-cc-pVTZ and aug*M*-cc-pVQZ results were used. Using the standard CBS-1 extrapolation, we obtain an MP2 detachment energy of −237 meV, ostensibly in the CBS limit. Subsequent extrapolations demonstrate that this erroneous value does not reflect an inherent deficiency of MP2: CBS-3 and CBS-4 extrapolations differ from one another by only 5 meV, with the latter only 18 meV below the experimental VDE.

It is encouraging that the MP2/aug*M*-cc-pV*N* Z detachment energy changes only slightly with increasing *N*, provided that three or four shells of diffuse functions are present. Double-ζ results for $M = 3$ and $M = 4$ are each <10 meV below the MP2/CBS-4 value, indicating that high angular momentum

TABLE 1: Calculated Vertical Electron Detachment Energies (VDEs) at the MP2/aug3-cc-pVDZ Optimized Geometry of *cis*-$(H_2O)_2^-$

	VDE (meV)					
basis set	BLYP	B3LYP	X3LYP	BHLYP	MP2	CCSD(t)
aug3-cc-pVDZ	177	132	67	−40	16	34
aug3-cc-pVTZ	184	147	63	−43	18	
aug3-cc-pVQZ	190	277	115	−42	20	
CBS-3	194	371	138	−42	22	
aug4-cc-pVDZ	276	256	199	51	26	42
aug4-cc-pVTZ	278	258	203	51	26	
aug4-cc-pVQZ	281	260	198	52	27	
CBS-4	284	262	195	53	27	
6-31(1+2+)G*	66	124	56	−76	−97	−83
6-31(1+3+)G*	167	208	149	29	17	27
6-31(1+4+)G*	243	241	188	56	32	42
6-31(2+2+)G*	104	160	92	−37	−51	−37
6-31(2+2+)G**	99	155	88	46	−58	−42
6-31(2+3+)G*	178	218	157	37	27	38
6-31(2+4+)G*	260	256	203	66	40	51
6-31(3+2+)G*	140	192	128	8	2	15
6-31(3+3+)G*	199	227	168	46	36	46
6-31(3+3+)G**	195	223	163	42	30	42
6-31(3+4+)G*	273	264	208	68	44	54
6-31(4+4+)G*	296	280	224	73	45	55
6-311(1+2+)G**	61	118	50	−81	−107	−88
6-311(1+3+)G**	158	200	140	20	7	19
6-311(2+3+)G**	167	207	147	27	15	29
6-311(2+3+)G(2*df*, *pd*)	158	199	138	19	12	27

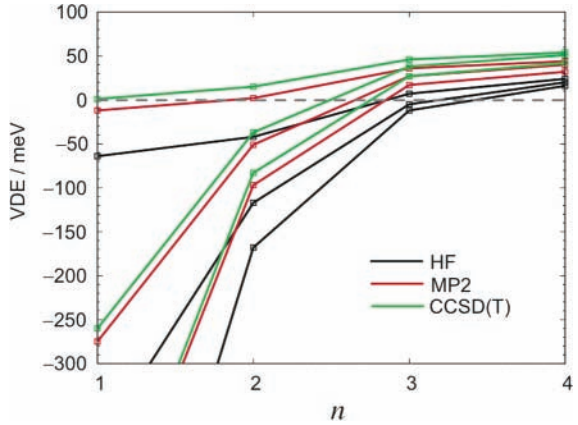

Figure 2. Calculated vertical electron detachment energies (VDEs) for $(H_2O)_2^-$, using the 6-31(m+n+)G* sequence of basis sets (m = 1, 2, 3).

functions are not important in VDE calculations. This supposition is corroborated by MP2 results in smaller, Pople-style basis sets: even 6-31(m+n+)G* affords VDEs near the MP2/CBS limit (Figure 1), provided that at least three sets of diffuse functions are present. Triple-ζ results fall 10−20 meV below the corresponding double-ζ values, whereas the addition of *f* functions for the O atoms and *d* functions for the H atoms decreases the VDE by less still (see Table 1).

It is noteworthy that the smallest exponent in the 6-31(1+3+)G* basis is 0.004 au, meaning that this basis is considerably *less* diffuse than those typically used to study $(H_2O)_2^-$. Exponents as small as 1.0×10^{-6} au are used routinely in dipole-bound anion calculations; however, our data indicate that this is excessive. The convergence that we observe can be rationalized as follows. Chen and Sheu[35] (who used a floating-center basis with exponents as small as 1.0×10^{-6} au) estimate that the radius of gyration (r_g) for the SOMO of *cis*-$(H_2O)_2^-$,

$$r_g = \langle \phi_{SOMO} | r^2 | \phi_{SOMO} \rangle^{1/2}$$

is ∼20 Å. Our "3+" *s* function on hydrogen has a full width at half-maximum (FWHM) of 14 Å, whereas a "4+" *s* function has a FWHM of 24 Å; thus, it makes sense that the VDE is essentially converged with the addition of 3−4 diffuse shells on the H atoms. To confirm this convergence beyond even unreasonable doubts, we repeated our MP2 and CCSD(T) calculations on $(H_2O)_2^-$, using a progression factor of $p = 1/5$ to define the diffuse shells, rather than the factor of $p = 1/3$ that was discussed in Section II. VDEs calculated using this modified 6-31(1+4+)G* basis differ by <1 meV from those obtained with our original 6-31(1+4+)G* basis, even though the latter is more diffuse by a factor of 4.6 in the smallest exponent.

Our best estimate (MP2/CBS-4) of the $(H_2O)_2^-$ VDE falls ∼20 meV below the experimental value, with the difference being attributable to correlation effects not captured with second-order perturbation theory. (In double-ζ Pople basis sets, MP2 converges, fortuitously, to the experimental VDE, but the addition of polarization functions drops the VDE back below experimental values.) Depicted in Figure 2 are CCSD(T)/6−31(n+m+)G* results, which closely track the corresponding MP2 values but are shifted to stronger binding by 10−20 meV. The fact that CCSD(T) binds the electron more strongly than MP2 is consistent with the notion that the former recovers a greater fraction of the correlation energy, which is larger for the anion than for the neutral cluster. At the double-ζ level, the converged CCSD(T) detachment energy is 55 meV, slightly higher than the experimental VDE, consistent with the observation that higher angular momentum basis functions engender a slight decrease in the VDE.

The performance of MP2 versus CCSD(T) for $(H_2O)_2^-$ is a marked contrast to the often unreliable results of open-shell MP2 for other radicals.[67,68] In particular, spin contamination is known to inhibit convergence of the Møller−Plesset perturbation series,[69−73] which is an effect that has been specifically noted in electron affinity (EA) calculations.[70] This is manifestly not a problem for water cluster anions, which are rather tame as far as radicals are concerned: typical $\langle \hat{S}^2 \rangle$ values in our calculations are in the range of 0.75−0.7508. (Absent tight thresholds, however, spuriously large values are sometimes observed in highly diffuse basis sets.) The unpaired electron in $(H_2O)_n^-$ is not strongly associated to any particular atom or water monomer and remains relatively far away from the valence electrons of the closed-shell water molecules, so that the unrestricted HF solution is qualitatively correct and correlation effects are small. Indeed, Figure 2 shows that the HF detachment energy for $(H_2O)_2^-$ converges smoothly to a value only ∼20 meV below the MP2 value and 30 meV below CCSD(T). If the detachment energy in this system were not so close to zero, electron correlation would be qualitatively unimportant.

Of course, errors on the order of a few tens of millielectron volts represent a substantial fraction of the actual VDE for a feebly bound anion, such as $(H_2O)_2^-$, and in such cases of extremely weak electron binding, correlation effects beyond fourth order in perturbation theory often provide the majority of the electron binding energy.[45,74−78] For such systems—including certain isomers of $(H_2O)_n^-$, discussed later in this work—it is impossible to determine, at the MP2 level, whether the anion is stable with respect to autodetachment. Nevertheless, the MP2 detachment energy plus its inherent uncertainty does establish a useful lower bound on the complete-basis, full configuration-interaction VDE. Thus, if MP2/6-31(1+3+)G* returns a VDE of, for example, −20 meV for a particular anion, one cannot say with certainty whether that anion is bound or not. However, one may conclude with certainty that the actual VDE is not large.

In contrast to wave function-based methods, all of which approach the experimental VDE from below as the basis set becomes increasingly diffuse, three of the four density functionals tested here are strongly overbinding at convergence. The exception is BHLYP, which affords VDEs that are only ∼10 meV higher than CCSD(T) results in the same basis set (Figure 3). This is not unprecedented: in studies of C_2F_n, SiF_n, and SF_n, King and co-workers[79−81] determined that BHLYP affords the lowest VDEs and EAs of any common density functional, although their explanation—that BHLYP predicts the shortest and most-accurate bond lengths—does not explain the present results, because we have used an MP2 geometry. In a recent, comprehensive review of calculated and experimental EAs,[82] BHLYP was the only functional that did *not* consistently overestimate these quantities, relative to the experimental results. On the other hand, the BHLYP prediction may fall above or below the experimental results, and its overall statistical error bars for EAs are larger than those of BLYP or B3LYP.[82]

It is also interesting to note from Figure 3 that VDEs calculated with B3LYP, X3LYP, and BLYP do not seem to have converged with the addition of four diffuse shells. For neutral species, DFT converges to the CBS limit much more

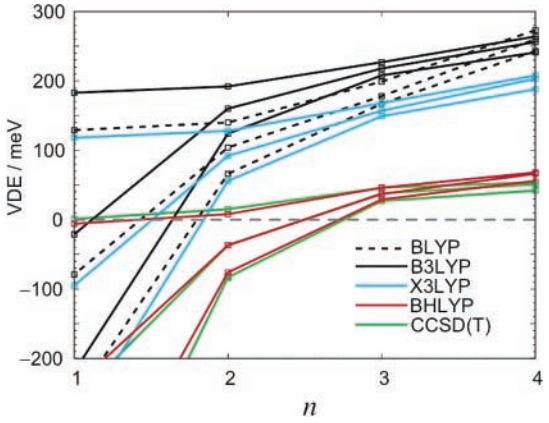

Figure 3. Calculated VDEs for $(H_2O)_2^-$ using the 6-31(m+n+)G* sequence of basis sets (m = 1, 2, 3).

rapidly than wave function methods; however, for anions, this is not always the case. In particular, for density functionals that are not rigorously free of self-interaction, only those anions that have extraordinarily large EAs can be expected to possess a well-defined CBS limit.[62,83] (In the case of BLYP, "extraordinarily large" seems to mean >3.4 eV.[62]) The DFT energy of an anion that is, in reality, only weakly bound may tend toward $-\infty$ in the CBS limit, whence the VDE approaches $+\infty$. The problem is mitigated, although not eliminated, through the use of functionals that incorporate HF exchange;[62] for the case of BHLYP (50% HF exchange) applied to $(H_2O)_2^-$, the divergence, if it exists, is pushed well beyond the size of basis sets that we are prepared to use.

Given the substantial empirical evidence that small-basis DFT provides reasonable structures, vibrational frequencies, and detachment energies for anions,[82] Jensen[62] has suggested that the selection of a small basis to avoid unphysical divergence represents simply another layer of parametrization in DFT. However, it is crucial to note that DFT *underbinds* the extra electron in small basis sets, as do wave function methods, but unlike wave function methods, DFT substantially *overbinds* the electron at convergence. Hence, there exists some artifactual régime in which the VDE obtained from DFT is fortuitously close to the experimental values. For example, the B3LYP/CBS-1 detachment energy for $(H_2O)_2^-$ is 18 meV, which is far superior to the MP2/CBS-1 estimate; however, further augmentation of the basis set reverses the situation. The all-too-common practice of haphazardly tinkering with the basis set until DFT agrees with experiment is especially dangerous for anions.

B. Water Trimer Anion. We performed a similar set of benchmark calculations for a linear and a cyclic isomer of the water trimer anion, each optimized at the MP2/6-311(2+3+)-G** level. These isomers are almost isoenergetic but exhibit quite different electron binding motifs and VDEs. The linear isomer, which is similar to that designated "$3L_{da}$" in ref 28 (and also studied elsewhere[23,31,32,36]), binds an electron via two dangling protons on a single terminal water molecule, whereas the cyclic isomer is similar to structure "$3R_{da}$" studied in ref 28 (and elsewhere[31,32,36]).

Just as we did for the dimer anion, in Figure 4 we plot sequences of calculated VDEs for $(H_2O)_3^-$ in increasingly diffuse Pople-style basis sets. (Numerical data are given in Table 2.) The linear isomer is believed to be the species probed in photodetachment experiments,[7,23,36] which yield experimental VDEs of 130 meV[8] and 142 meV.[84] Our best calculation, CCSD(T)/6−311(2+3+)G**, pinpoints the latter of these, at

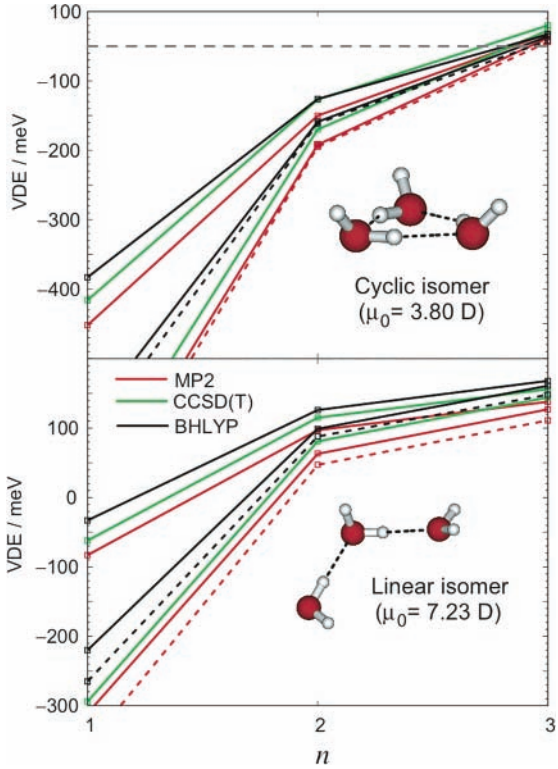

Figure 4. Calculated VDEs for isomers of $(H_2O)_3^-$ in 6-31(m+n+)G* basis sets (solid lines) and the 6-311(1+n+)G** basis sets (broken lines), for m = 1 and m = 2. Dipole moments μ_0 are MP2/6-311(2+3+)G** values for the neutral cluster at the same geometry.

141 meV, undoubtedly the result of a cancellation of the effects of additional diffuse functions (which would increase the VDE slightly) and that of higher angular momentum functions (which have a tendency to decrease it). MP2 estimates lie no more than 20 meV below the corresponding CCSD(T) values, whereas the BHLYP predictions err by roughly the same amount in the opposite direction. The other three density functionals overestimate the VDE by 100−200 meV.

Three sets of H-atom diffuse functions seem to be sufficient to converge the VDE of the linear isomer to within a few tens of millielectron volts; however, for the feebly binding cyclic isomer, the fourth set of H-atom diffuse functions contributes 30−40 meV to the VDE. At the MP2 level, this isomer does not bind the extra electron unless four sets of diffuse shells are present (see Table 2). Our experience indicates that the addition of a fourth set of diffuse functions per atom greatly exacerbates convergence difficulties in Pople-style basis sets. (Such problems manifest even sooner in Dunning-style basis sets.) As such, to converge the VDEs of the most weakly bound isomers of $(H_2O)_n^-$, it is advisable to vary the progression factor that defines the diffuse shells. For most of our calculations, this progression factor was fixed (a priori and somewhat arbitrarily) to be $p = {}^1/_3$; however, in Figure 5, we compare MP2/ and CCSD(T)/6−31(m+n+)G* results using progression factors of $p = {}^1/_3$, ${}^1/_5$, and ${}^1/_8$. All of the results are almost coincident after four diffuse shells have been incorporated; however, the sequences with progression factors of $p = {}^1/_5$ and $p = {}^1/_8$ converge after three shells rather than four shells. Therefore, a progression factor of $p \approx {}^1/_5$ is recommended when targeting isomers that have VDEs near zero.

In addition to electron detachment energies, one must be concerned with the convergence of relative energies of cluster isomers. Listed in Table 2 are zero-point-corrected relative

TABLE 2: VDEs and Zero-Point-Corrected Relative Energies for Two Isomers of $(H_2O)_3^-$ at Their Respective MP2/6−311(2+3+)G Geometries.**

	VDE (meV)						
	Cyclic		Linear		D_0(cyclic) − D_0(linear) (kcal/mol)		
basis set	MP2	CCSD(T)	MP2	CCSD(T)	B3LYP[a]	MP2[b]	CCSD(T)[b]
aug3-cc-pVDZ	−28	−12	112	142		−0.63	−0.27
aug3-cc-pVTZ	−23		112			−0.77	
aug3-cc-pVQZ	−133		114			1.82	
CBS-3	−214		115				
6-31(1+2+)G*	−192	−170	63	81	1.38	1.53	1.56
6-31(1+3+)G*	−38	−27	127	144	1.05	−0.56	−0.29
6-31(1+4+)G*	−2	4	128	147	0.91	−1.37	−0.95
6-31(2+2+)G*	−150	−127	97	115	1.32	1.19	1.22
6-31(2+3+)G*	−32	−20	138	156		−0.60	−0.34
6-31(2+4+)G*	0	8	138	159	0.73	−1.34	−0.93
6-311(1+2+)G**	−195	−168	47	78	2.00	2.14	2.09
6-311(1+3+)G**	−44	−31	111	132	1.48	0.14	0.35
6-311(2+1+)G**	−442	−399	−91	−62	2.53	4.67	4.39
6-311(2+2+)G**	−159	−132	74	98		1.92	1.90
6-311(2+3+)G**	−39	−25	119	141	1.34	0.21	0.41

[a] Uses the B3LYP harmonic zero-point energy in each particular basis set. [b] Uses the MP2/6-311(2+3+)G** harmonic zero-point energy (1.16 kcal/mol greater for the cyclic isomer than for the linear isomer).

TABLE 3: Calculated VDEs and Relative Energies (E)[a] for Isomers of $(H_2O)_4^-$ Optimized at Different Levels of Theory

	Isomer A		Isomer B		Isomer C		Isomer D	
single points	VDE (meV)	E (kcal/mol)	VDE (meV)	E (kcal/mol)	VDE (meV)	E (kcal/mol)	VDE (meV)	E (kcal/mol)
				B3LYP/6-31(1+1+)G* Geometry				
B3LYP[b]	678	2.04	518	2.01	370	0.00	601	2.19
BHLYP[b]	467	4.57	305	4.18	182	0.00	394	4.52
MP2[b]	376	1.67	221	1.70	108	0.00	332	1.38
CCSD(T)[b]	407	1.25	225	2.08	138	0.00	336	1.64
				B3LYP/6-311(1+1+)G** Geometry				
B3LYP[b]	658	1.98	501	1.92	363	0.00	583	2.08
BHLYP[b]	451	4.32	291	3.85	175	0.00	378	4.20
MP2[b]	366	1.51	218	1.43	103	0.00	293	1.90
CCSD(T)[b]	395	1.18	248	1.27	132	0.00	323	1.62
				B3LYP/6-31(1+3+)G* Geometry				
B3LYP[b]	644	2.85	481	2.78	258	0.00	535	2.88
BHLYP[b]	343	6.50	270	5.90	76	0.00	327	6.11
MP2[b]	350	3.63	199	3.47	40	0.00	250	3.65
CCSD(T)[b]	380	2.73	229	2.77	60	0.00	280	2.89
				B3LYP/6-31(1+3+)G** Geometry				
B3LYP[b]	620	2.81	457	2.72	211	0.00	500	2.82
BHLYP[b]	414	6.80	250	6.10	35	0.00	295	6.32
MP2[b]	336	3.96	184	3.82	12	0.00	225	3.99
CCSD(T)[b]	364	3.03	213	3.10	29	0.00	254	3.23
				B3LYP/6-31(1+1+)G*-f(3+) Geometry				
B3LYP[c]	553	2.44	371	2.96	208	0.00	468	2.75
BHLYP[c]	363	5.47	165	5.66	43	0.00	272	5.57
MP2[c]	314	3.31	110	4.02	62	0.00	213	3.99
CCSD(T)[c]	343	2.54	145	3.33	83	0.00	245	3.27
				MP2/6-31(2+3+)G** Geometry				
B3LYP[b]	607	2.70	443	2.56	173	0.00	483	2.71
BHLYP[b]	404	7.00	238	6.25	1	0.00	281	6.45
MP2[b]	332	4.08	177	3.96	−13	0.00	217	4.12
CCSD[b]	345	2.94	193	3.00	−4	0.00	232	3.15
CCSD(T)[b]	359	3.09	204	3.18	1	0.00	244	3.30
				Experiment[d]				
	350		250		60			

[a] Not including zero-point corrections. [b] 6-31(1+3+)G* basis. [c] 6-311(1+1+)G**-f(3+) basis. [d] Experimental VDEs and their assignments are taken from ref 9.

energies (D_0) of the linear and cyclic isomers of $(H_2O)_3^-$ at selected levels of theory. Probably the most reliable structural calculations on water trimer anion are those of Kim et al.,[28] whose $3R_{da}$ (cyclic) isomer has the lowest D_0 value of the eight isomers considered in that work, whereas their $3L_{da}$ (linear) isomer lies 0.8 kcal/mol higher in energy, in good agreement with our best estimate of 0.4 kcal/mol. Neither of these calculations uses any f functions and neither can claim an accuracy of 1 kcal/mol; however, the trend that is apparent from Table 2 seems to indicate that the cyclic isomer will, indeed, be slightly more stable in the CBS limit. Two competing basis-set effects are also evident: on one hand, a more-diffuse

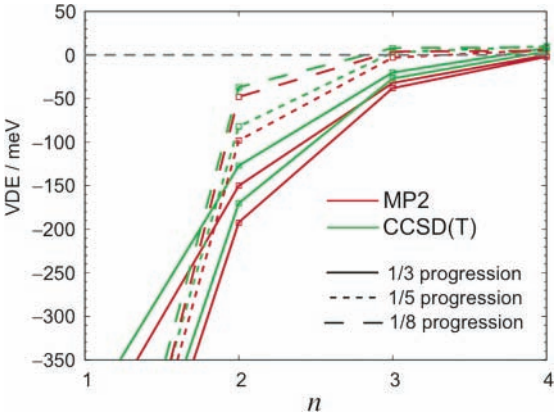

Figure 5. Calculated VDEs for cyclic $(H_2O)_3^-$ in 6-31(m+n+)G* basis sets, with a diffuse-exponent progression factor of $p = 1/3$ (solid lines, depicted for $m = 1$ and $m = 2$), $p = 1/5$ (short dashes, depicted for $m = 1$ only), and $p = 1/8$ (long dashes, depicted for $m = 1$ only).

basis favors the cyclic isomer over the linear structure, because the former's electron density is more diffuse, but the addition of higher angular momentum functions enhances the relative stability of the linear isomer. Both effects are much larger than the difference in relative energies and also much larger than the difference between MP2 and CCSD(T) relative energies. Although Kim and co-workers[28,31] argue that coupled-cluster methods are indispensable for ascertaining the most-stable isomer, in this case, it is primarily a basis-set effect and not a correlation effect that determines which isomer is more stable. Certainly, coupled-cluster theory is necessary to quantify the energy difference precisely; however, even B3LYP correctly reproduces the trend in relative energies, as a function of the basis set.

Our results for $(H_2O)_2^-$ and $(H_2O)_3^-$ demonstrate that VDEs converge to the CBS limit much more rapidly than isomeric energy differences do. If we were to calculate VDEs for ionization of neutral water clusters, very large basis sets would be required to reach the CBS limit, because the removal of a valence electron engenders significant relaxation of the wave function, such that little or no cancellation of errors would be expected between the cationic and the neutral cluster energies. Thus, energy differences ordinarily do not converge to the CBS limit any faster than absolute energies.[85,86] For a dipole-bound anion, however, the most weakly bound electron resides beyond the valence shell of the neutral molecule or cluster that supports it; therefore, the electronic structure of the anion's neutral core is much the same as that in the bare neutral, which leads to significant cancellation of basis-set effects in the VDE calculation.

C. Water Tetramer Anion. We now consider the four isomers of $(H_2O)_4^-$ that are depicted in Figure 6. Our notation for isomers A−C follows that of Shin et al.,[9] who assigned these isomers to peaks in the photoelectron spectrum, using existing CCSD calculations for a slew of different isomers.[31,87] Isomer D in Figure 6 was not considered; however, it is structurally and energetically similar to the other three isomers. Depicted in Figure 7 is the familiar plot illustrating basis-set convergence of the calculated VDEs for isomers A and C. These calculations use B3LYP/6-31++G* geometries that do not suffice to reproduce the experimental detachment energies; nevertheless, the convergence of the calculated VDEs is quite similar to that observed for the dimer and trimer anions. Relative to CCSD(T), the functionals BLYP, B3LYP, and X3LYP overbind the electron by 200−300 meV in all four isomers, with errors tending to be slightly larger for the more strongly bound isomers.

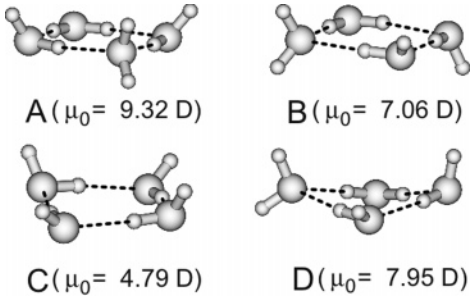

Figure 6. Isomers of $(H_2O)_4^-$ considered in this work, along with MP2/6-311(2+3+)G** dipole moments for the corresponding neutral clusters.

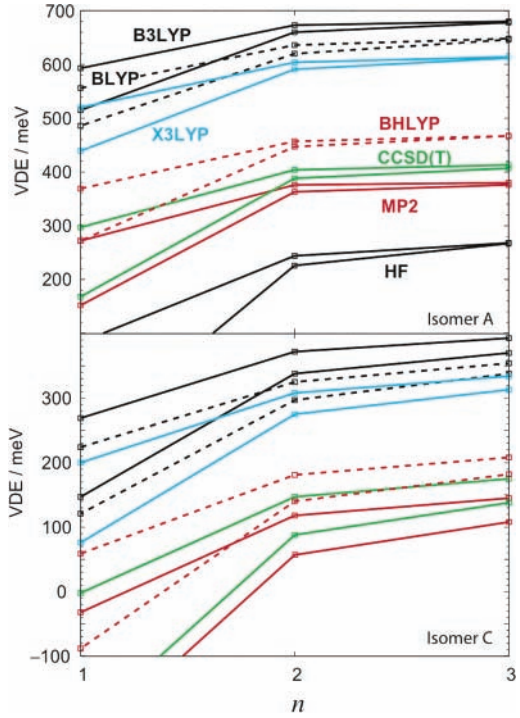

Figure 7. Calculated VDEs for isomers of $(H_2O)_4^-$ using 6-31(m+n+)G* basis sets ($m = 1$ and 2).

MP2 consistently underestimates the VDE by ∼30 meV and BHLYP typically errs by a slightly larger amount in the other direction, although, for some basis sets, the BHLYP detachment energy is less than the CCSD(T) detachment energy.

In Table 3, we study the convergence of the VDE versus the method of geometry optimization. Consistent with the assignment of Shin et al.,[9] our best calculation [CCSD(T)/6-31(1+3+)G*//MP2/6−311(2+3+)G**] reproduces the position of the dominant peak in the photoelectron spectrum to within 9 meV. Our calculations are also consistent, within the limitations of our basis sets, with the assignment of isomer C to the weak spectral feature at 60 meV. [Using a progression factor of $p = 1/5$ rather than $p = 1/3$ to define the 6-31(1+3+)G* basis results in a CCSD(T) detachment energy of 22 meV for isomer C, which is more similar to the experimental result but still 40 meV too small.] Finally, our calculations indicate that the secondary peak in the photoelectron spectrum, at 250 meV, probably results from a combination of isomers B and D, whereas, previously, this feature was assigned exclusively to isomer B.[9]

With an eye toward larger clusters, let us also now consider the effect of geometry optimizations that are performed at lower levels of theory, namely, B3LYP in modest basis sets. In this

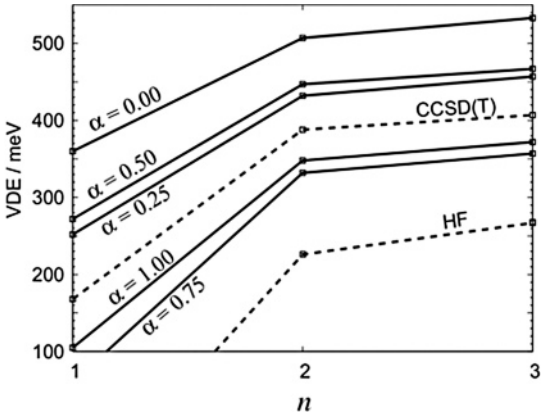

Figure 8. Calculated VDEs for isomer A of $(H_2O)_4^-$ in 6-31(1+*n*+)G* basis sets, using the functional E_α defined in the text.

case, VDEs converge toward the experimental values from above as the size and diffuseness of the basis set is increased (see Table 3). CCSD(T)/6-31(1+3+)G* detachment energies calculated at B3LYP/6-311(1+3+)G** geometries are within 10 meV of those at the MP2 geometry for all isomers except isomer C, where the difference is almost 30 meV. MP2 detachment energies exhibit similar convergence as a function of geometry. We also acknowledge the fact that it is possible to reproduce the experimental VDEs for this cluster using a relatively modest atom-centered basis combined with a single floating center equipped with three sets of diffuse functions. In particular, the floating-center calculations give a much more accurate value for the VDE of isomer C.

For the dimer, trimer, and tetramer anions, BHLYP detachment energies are consistently and significantly more accurate than those of other common density functionals, regardless of cluster geometry. We have no good explanation for why this is the case, although the role of HF exchange is a likely candidate, insofar as the coefficient of HF exchange in BHLYP is larger than that in any of the other three functionals. To evaluate the role of HF exchange in the prediction of VDEs, let us define a new functional,

$$E_\alpha = \alpha E_X^{HF} + (1-\alpha)E_X^{Slater} + E_C^{LYP}$$

with a single adjustable parameter α, which is the coefficient of HF exchange. When $\alpha = 0.5$, E_α is exactly BHLYP. VDE predictions for isomer A of $(H_2O)_4^-$ are plotted in Figure 8 for several values of α. The trend is toward a lower VDE as α increases, though not in strictly monotone fashion. It is interesting and potentially useful to note that the VDEs for $\alpha = 0$ and $\alpha = 1$ bracket the CCSD(T) value, potentially providing a cost-effective way to obtain rough estimates of VDEs in large clusters.

D. Clusters of Intermediate Size: $(H_2O)_6^-$ and $(H_2O)_{12}^-$. To establish continuity between our conclusions for the dimer through tetramer, studied previously, and the large water clusters discussed subsequently, in this section, we briefly visit the intermediate size régime, as exemplified by $(H_2O)_6^-$ and $(H_2O)_{12}^-$. For the former, CCSD(T)/6−31(1+3+)G* calculations are still feasible, and in Table 4, we compare these benchmark VDEs to those calculated at the MP2 and DFT levels, for the three isomers illustrated in Figure 9. [Until this point, all of the $(H_2O)_n^-$ isomers that we have considered are proper local minima; however, beginning with the hexamer, we no longer calculate vibrational frequencies. Therefore, some of these larger clusters may represent saddle points on the $(H_2O)_n^-$ potential surface, but this is inconsequential to our analysis of VDEs. In addition, from this point forward, we switch from meV to eV, as the larger clusters may have VDEs in excess of 1 eV.]

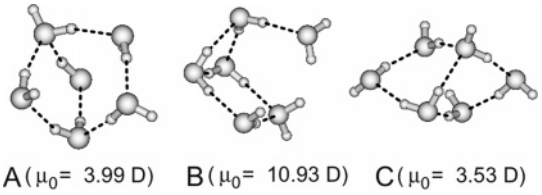

Figure 9. X3LYP/6-31++G* optimized geometries for isomers of $(H_2O)_6^-$, along with X3LYP/6-311++G** dipole moments of the corresponding neutral clusters.

TABLE 4: Calculated VDEs for Cagelike Isomers of $(H_2O)_6^-$ (Optimized at the X3LYP/6-31++G* Level), Using the 6-31(1+3+)G* Basis with Two Different Progression Factors (*p*)

	VDE (eV)				
	Isomer A		Isomer B	Isomer C	
method	$p = 1/3$	$p = 1/5$	$p = 1/3$	$p = 1/3$	$p = 1/5$
CCSD(T)	0.061	0.066	0.740	0.004	0.019
MP2	0.031	0.038	0.706	−0.019	0.003
BHLYP	0.085	0.099	0.905	0.018	0.038
BLYP	0.307	0.362	1.095	0.233	0.290
B3LYP	0.294	0.327	1.115	0.227	0.247
X3LYP	0.241	0.273	1.047	0.172	0.203

The $(H_2O)_6^-$ isomers depicted in Figure 9 were selected to compare species that bind the electron strongly (isomer B) to those that bind the electron rather weakly (isomers A and C), and, for isomers A and C, we compare VDEs using two different progression factors to define the 6-31(1+3+)G* basis. At the MP2 and CCSD(T) levels, the progression factor $p = 1/5$ increases the VDEs by 20 meV or less, as compared to $p = 1/3$, which is a difference only half as large as that observed for cyclic $(H_2O)_3^-$ (cf. Figure 5), which is reasonable because the latter has a VDE of almost zero. The difference between the two progression factors for $(H_2O)_6^-$ is more pronounced at the DFT level, especially for BLYP, which is consistent with our earlier remarks regarding the slow convergence—and possible divergence—of DFT energies for weakly bound anions (see Section III.A). With regard to the VDEs themselves, the functionals BLYP, B3LYP, and X3LYP overestimate the VDE of isomers A and C by 200−300 meV, whereas BHLYP is an order of magnitude closer to CCSD(T). As with the tetramer anion, the DFT overbinding grows larger in magnitude as the VDE increases, and for isomer B of $(H_2O)_6^-$, even BHLYP is 165 meV above CCSD(T). In contrast, the difference between MP2 and CCSD(T) remains consistent at 20−30 meV across all three isomers. [The experimental VDE for $(H_2O)_6^-$ is 450 meV,[7] which is significantly lower than that of isomer B, which is not surprising, because isomer B is ∼8 kcal/mol higher in energy than isomer A and is unlikely to be formed in a molecular beam. However, this fact has no bearing on our analysis of VDE convergence.]

In Figure 10, we plot VDE convergence in 6-31(1+*n*+)G* basis sets for two different isomers of $(H_2O)_{12}^-$. Isomer A is an edge-sharing hexagonal prism whose corresponding neutral cluster has essentially zero dipole moment, and VDEs for this species converge slowly to zero. Cleaving three hydrogen bonds on one face of isomer A, one obtains (following geometry optimization) isomer B, in which the excess electron is bound as a nascent "internalized" state that exhibits a larger VDE than

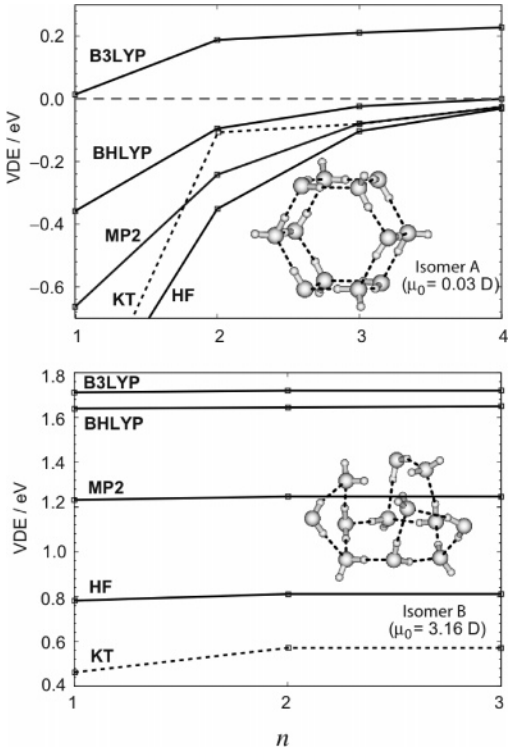

Figure 10. Calculated VDEs for X3LYP/6-31++G* optimized geometries of $(H_2O)_{12}^-$ in 6-31(1+*n*+)G* basis sets, along with X3LYP/6-311++G** dipole moments for the corresponding neutral clusters.

any cluster anion we have heretofore examined, despite the fact that the dipole moment of the underlying neutral cluster is smaller even than that in the case of the water dimer anion (3.16 D versus 4.65 D, at the same level of theory). Because of its strong binding, VDEs for isomer B of $(H_2O)_{12}^-$ are essentially converged with only a single set of diffuse functions.

Figure 10 also plots the Koopmans' theorem (KT) value of the VDE. The smooth convergence of this quantity, even for the unbound isomer A of $(H_2O)_{12}^-$, lends credence to the notion that the quality of the HF reference does not deteriorate seriously as the cluster size increases, and thus the MP2 detachment energies are probably reasonable. As with the smaller clusters, BLYP, B3LYP, and X3LYP severely overestimate the VDEs for both isomers of $(H_2O)_{12}^-$; however, the more interesting case is BHLYP, which overestimates the detachment energy only by ~30 meV (relative to MP2) for isomer A but by ~300 meV for the more strongly bound isomer B of $(H_2O)_{12}^-$.

E. Large Clusters: $(H_2O)_{20}^-$ and $(H_2O)_{24}^-$. Because of their role as building blocks of clathrate hydrates,[88] much attention has been devoted to neutral water clusters that consist of 20−28 monomers with high-symmetry polyhedral arrangements of O atoms.[89,91−96] Khan[40−42] examined the anionic analogues of several such clusters, mostly at the B3LYP/6-311++G** level, and claims to have identified the particular isomers responsible for the photoelectron spectra of $(H_2O)_{20}^-$, $(H_2O)_{21}^-$, and $(H_2O)_{24}^-$. Although Khan postulates[41,42] that DFT detachment energy predictions should become more reliable as cluster size increases, Rienstra-Kiracofe et al.[82] specifically addressed this issue in their comprehensive review of density functional EA calculations, and found no evidence whatsoever to substantiate such a trend. In view of the significant overbinding exhibited by B3LYP in smaller clusters, we wish to assess the reliability of these large-cluster results using MP2 calculations. Because of the myriad of isomers available to such a large number of monomers, we limit our investigation to a few polyhedral-type isomers in the vein of those studied previously. With one exception, which is noted below, all geometries in this section were optimized at the X3LYP/6-31++G* level, which, if our results for the tetramer anion are any indication, is *not* sufficient to obtain VDEs in agreement with the experimental results. However, it does provide a set of reasonable geometries at which we can benchmark DFT versus MP2 detachment energies, and also furnishes a starting point from which to examine relationships between cluster geometry and VDE. No point-group symmetry was enforced in these geometry optimizations.

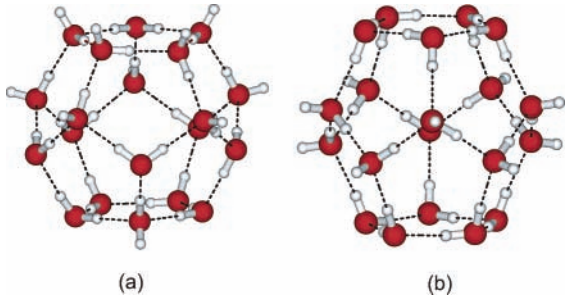

Figure 11. Representative examples of pentagonal dodecahedral (5^{12}) isomers of $(H_2O)_{20}^-$: (a) isomer A and (b) isomer F.

For $(H_2O)_{20}^-$, we began with six optimized geometries for the neutral cluster obtained from ref 89. One of these exhibits a $4^4 5^4 6^2$ topology[88] in its O-atom framework (i.e., four four-membered rings, four five-membered rings, and two six-membered rings of O atoms, all of which are connected by hydrogen bonds), whereas the others possess dodecahedral 5^{12} topologies. Representative examples of the 5^{12} isomers are illustrated in Figure 11. All six isomers possess 10 dangling protons, located at various positions around the cluster. In certain cases, an asymmetrical distribution of dangling protons results in an enormous dipole moment (see Table 5), making it at least plausible that a neutral 5^{12} cluster formed in a molecular beam might directly capture an electron to form $(H_2O)_{20}^-$ (although large-basis MP2 calculations place dodecahedral $(H_2O)_{20}$ isomers 12−18 kcal/mol above other isomeric families[90]).

Optimized geometries for $(H_2O)_{20}^-$ were obtained starting from each of the aforementioned $(H_2O)_{20}$ isomers. Because these isomers each bind the excess electron at the surface of the cluster, the additional electron does not alter the hydrogen-bonding network substantially, and, consequently, each of the optimized anion geometries is quite similar to the starting neutral cluster geometry.

Listed in Table 5 are VDEs for the $(H_2O)_{20}^-$ isomers and VAEs for the isomers of $(H_2O)_{20}$. (Recall that a negative VAE implies that the anion is lower in energy at the same geometry.) Because these particular cluster isomers exhibit large dipole moments and strong electron binding, convergence of the MP2 calculations, with respect to diffuse shells, is even faster than that observed for small clusters, and our best results [MP2/6-31(1+3+)G*] indicate that the overbinding exhibited by DFT in small clusters is somewhat more acute in the present case, which is consistent with our earlier conclusion that DFT overbinds the electron most severely for isomers that have large VDEs. The mean difference between the DFT/6-31(1+3+)G* and MP2/6-31(1+3+)G* detachment energies is 0.399 ± 0.031 eV for B3LYP, 0.453 ± 0.039 eV for BLYP, 0.349 ± 0.029 eV for X3LYP, and 0.154 ± 0.074 eV for BHLYP, where the reported uncertainties represent one standard deviation.

TABLE 5: Calculated Vertical Attachment Energies (VAEs) for Isomers of $(H_2O)_{20}$ and VDEs for Isomers of $(H_2O)_{20}^-$ (both in eV) at Various X3LYP/6-31++G* Optimized Geometries

		B3LYP				MP2	
isomer	μ_0/D[a]	6-311++G**	6-31(1+3+)G*	BLYP[b]	BHLYP[b]	6-31(1+2+)G*	6-31(1+3+)G*
$4^45^46^2$	4.85	−0.160	−0.333	−0.414	−0.077	0.100	0.000
5^{12} A	25.22	−1.122	−1.238	−1.281	−0.995	−0.803	−0.804
5^{12} B	17.82	−0.864	−0.987	−1.032	−0.747	−0.580	−0.584
5^{12} C	13.45	−0.617	−0.753	−0.807	−0.509	−0.359	−0.369
5^{12} D	13.74	−0.528	−0.677	−0.732	−0.430	−0.276	−0.265
5^{12} E	1.82	−0.193	−0.358	−0.453	0.066	0.180	0.045
$(4^45^46^2)^-$	6.34	0.286	0.437	0.512	0.181	0.025	0.074
$(5^{12})^-$ A	27.93	1.416	1.517	1.545	1.285	1.085	1.085
$(5^{12})^-$ B	21.21	1.201	1.307	1.327	1.084	0.910	0.910
$(5^{12})^-$ C	16.58	0.932	1.048	1.073	0.818	0.658	0.658
$(5^{12})^-$ D	16.05	0.779	0.903	0.940	0.668	0.512	0.516
$(5^{12})^-$ E	2.27	0.266	0.417	0.516	0.111	−0.139	−0.028
$(5^{12})^-$ F[c]	0.05	0.807	0.907	1.025	0.558	0.223	0.229

[a] B3LYP/6-311++G** dipole moment of the neutral cluster. [b] 6-31(1+3+)G* basis with a progression factor of $p = 1/3$. [c] Optimized at the B3LYP/6-31G* level, following ref 40.

Because 6-311++G** is often regarded as a "high-quality" basis in the context of density functional calculations, it is notable that VDEs and VAEs obtained using DFT in this basis are not converged with respect to the addition of diffuse shells, just as we observed for smaller clusters. The average difference between the 6-31(1+3+)G* and 6-311++G** VDEs is 0.134 ± 0.023 eV for B3LYP, 0.102 ± 0.010 for X3LYP, and 0.139 ± 0.024 eV for BLYP. These are significant increases that, had we satisfied ourselves with DFT/6-311++G** calculations, would have partially camouflaged the overbinding exhibited by these functionals.

The fact that BHLYP continues to afford VDEs that are relatively similar to MP2 values lends additional credibility to the latter estimates, in our opinion. The electronic structure of these $(H_2O)_{20}^-$ isomers is quite similar to that of the small clusters studied previously, where the SOMO resides on one end of the dipole moment vector and interacts strongly with two or three dangling protons. Therefore, we believe that these MP2 calculations are the most accurate VDE calculations to date for $(H_2O)_{20}^-$. Even a more conservative estimate—taking MP2 as a lower bound and BHLYP as an upper bound for the VDEs (*vice versa* for the VAEs)—yields a range of 0.2 eV or less for all but one of the isomers in Table 5. The outlier, 5^{12} isomer F, has essentially no dipole moment and, in this case, the MP2 prediction may err toward underbinding more so than for the other isomers.

Even so, the VDEs calculated here cast significant doubt upon the assignment of the $(H_2O)_{20}^-$ photoelectron spectrum made[40]—and, subsequently, made again[42]—by Khan. Photoelectron spectra for this species afford VDEs of 1.11 eV[14] and 1.18 eV,[20] which Khan[40] originally attributed to what we call 5^{12} isomer F, in which all 10 dangling protons are arranged about the equator, as illustrated in Figure 11b. We have reproduced both Khan's geometry optimization and his VDE calculation for this species (B3LYP/6-311++G**//B3LYP/6-31G*), obtaining a VDE of 0.807 eV, in comparison to Khan's value of 0.805 eV.[40] However, the MP2/6-31(1+3+)G* VDE at the same geometry is only 0.229 eV, whereas our results for $(H_2O)_4^-$ indicate that both the MP2 and the B3LYP detachment energies converge *from above* as the geometry optimization is improved. More recently, Khan reported a new isomer of $(H_2O)_{20}^-$ with a VDE of 1.32 eV[42] (B3LYP/aug-cc-pVDZ//B3LYP/6-311++G**). This is an internal (cavity) state of the excess electron, with enough distortion from high symmetry to make it difficult for us to reproduce his calculation exactly, and we have not considered cavity states of $(H_2O)_{20}^-$. Khan's VDE for this species exceeds the experimental values by 0.14−0.21 eV but, based on our assessment of DFT detachment energies, is probably ∼0.4 eV too large. Geometry optimization with additional diffuse functions would likely move Khan's VDE closer to experiment and, therefore, we cannot discount his assignment at present. Further investigation using MP2 is warranted.

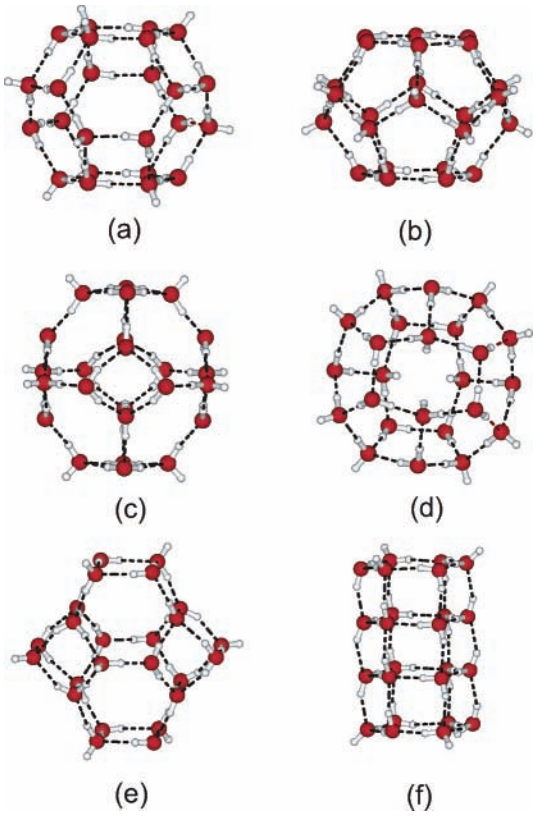

Figure 12. Representative examples of $(H_2O)_{24}^-$ isomers.

Last, we consider several isomers of $(H_2O)_{24}$ and $(H_2O)_{24}^-$, this time focusing on clusters with small dipole moments. This is, by no means, an exhaustive investigation, but several important structural motifs have been considered. These include variants of the 4^66^8 and $5^{12}6^2$ tetradecahedrons, shown in Figure 12a and b, respectively, which, in their neutral forms, are building blocks of clathrate hydrates.[89,94,96] Similar to the 5^{12} clusters considered previously, these clusters have many outward-

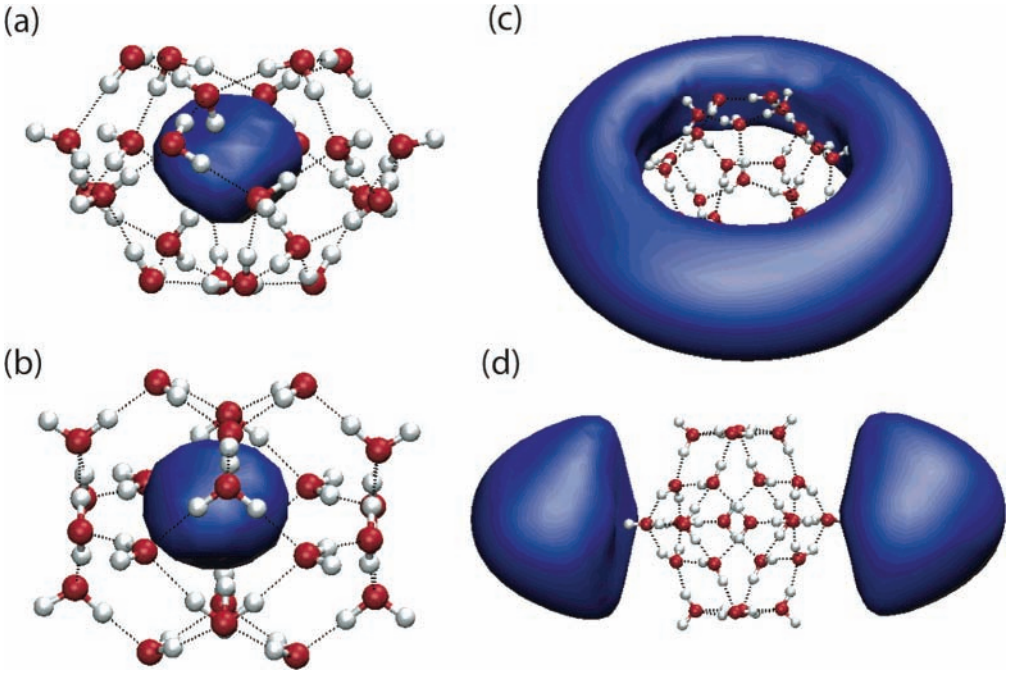

Figure 13. HF/6-31(1+3+)G* SOMOs for isomers of $(H_2O)_{24}^-$, illustrating (a) isomer $(5^{12}6^2)^-$ B, (b) isomer $(4^66^8)^-$ B, (c) isomer $(5^{12}6^2)^-$ C, and (d) isomer $(4^{14}6^4)^-$ A. Cavity states are plotted with a contour of 0.035 au; surface states use a contour of 0.005 au.

TABLE 6: Calculated VAEs for Isomers of $(H_2O)_{24}$ and VDEs for Isomers of $(H_2O)_{24}^-$ (both in eV) at Various X3LYP/6-31++G* Optimized Geometries

			B3LYP				MP2[d]	
isomer	state[a]	μ_0/D[b]	6-311++G**	6-31(1+3+)G*	X3LYP[c]	BHLYP[c]	$p = 1/3$	$p = 1/5$
(4^66^8)		0.00	−0.095	−0.260	−0.239	−0.007	0.079	
$(4^{14}6^4)$ A		0.00	−0.293	−0.439	−0.403	0.133	0.014	
$(4^{14}6^4)$ B		0.01	−0.229	−0.387	−0.349	0.082	0.037	
$(5^{12}6^2)$ A	(ss)	0.05	−0.558	−0.684	−.645	−0.336	−0.089	
$(5^{12}6^2)$ B		0.28	−0.198	−0.349	−0.319	0.046	0.066	
$(5^{12}6^2)$ C	(ss)	5.01	−0.400	−0.523	−0.482	−0.192	−0.065	
$(5^{12}6^2)$ D		4.88	−0.411	−0.519	−0.487	−0.210	0.014	
(4^{14})		0.00	−0.163	−0.322	−0.290	−0.025	0.068	
$(4^66^8)^-$ A		0.00	0.135	0.287	0.267	0.010	−0.078	−0.032
$(4^66^8)^-$ B	(is)	0.00	0.992	1.039	0.989	0.862	0.576	
$(4^{14}6^4)^-$ A	(ss)	0.00	0.503	0.598	0.445	0.171	0.001	0.008
$(4^{14}6^4)^-$ B		0.00	0.660	0.733	0.611	0.421	−0.001	0.007
$(5^{12}6^2)^-$ A		0.39	0.260	0.400	0.367	0.079	−0.060	
$(5^{12}6^2)^-$ B	(is)	0.01	1.216	1.262	1.205	1.099	0.795	0.796
$(5^{12}6^2)^-$ C	(ss)	0.02	0.684	0.796	0.755	0.430	0.138	0.130
$(4^{14})^-$		0.00	0.208	0.351	0.323	0.047	−0.068	0.027

[a] SOMOs of stable anions are classified as either surface states (ss) or interior states (is). [b] B3LYP/6-311++G** dipole moment of the neutral cluster. [c] 6-31(1+3+)G* basis with progression factor of $p = 1/3$. [d] 6-31(1+3+)G* basis with two different progression factors p.

pointing dangling protons that support surface states of the excess electron. In contrast to the 20-mer clusters that we considered, however, these $(H_2O)_{24}^-$ isomers have negligible dipole moments and the SOMOs are, in some cases, delocalized over much of the surface of the cluster, as, for example, in Figure 13b. When one or more dangling protons are rotated into the interior of the cavity, tetradecahedral clusters can stabilize the excess electron internally; panels c and d in Figure 12 depict two such isomers, which result from the depictions shown in panels a and b in Figure 12, respectively, when four dangling protons are rotated into the interior. Typical SOMOs for these cavity isomers are depicted in Figure 13a and b. Finally, we consider examples of $4^{14}6^4$ edge-sharing prismatic structures, such as that shown in Figure 12e, and 4^{14} face-sharing prismatic (also known as fused-cubic or box-kite) structures, such as that in Figure 12f. The latter we include because empirical water potentials consistently predict that $(H_2O)_{24}$ has a fused-cubic global minimum.[97] Certain members of this group of isomers support SOMOs that are localized on a few dangling H atoms, as, for example, in Figure 13d, rather than delocalized over the entire surface of the cluster. This particular surface state consists of two lobes of charge localized on opposite sides of the cluster; however, small changes in the cluster geometry cause the SOMO to localize on one side or the other.

Calculated VAEs and VDEs for these isomers are listed in Table 6. The spread between BHLYP and MP2 values is larger here than for the 20-mer, in the range of 0.3−0.4 eV in several cases, although considerably narrower for other isomers. The magnitude of the difference does not seem to be dependent on the nature of excess electron solvation (surface state versus internal state), and the larger range of differences observed here probably reflects the greater diversity of isomers chosen for this system.

At the MP2/6-31(1+3+)G* level, the most strongly bound of our $(H_2O)_{24}^-$ isomers is the internal state whose geometry is depicted in Figure 12d; however, the calculated VDE (0.795 eV) is significantly smaller than experimental values (1.30 eV[3,20] and 1.19 eV[14]). We feel that this rules out this isomer as being the one responsible for the photoelectron spectrum. A comparable four-coordinate $5^{12}6^2$ cavity state, with a calculated VDE of 1.35 eV (B3LYP/6-311++G**//B3LYP/6-31G* level), has been proposed by Khan to be the experimentally observed isomer;[41] however, our calculations cast doubt on this assignment, because the B3LYP/6-311++G** VDE for the isomer in Figure 12d is 1.216 eV, or 0.421 eV higher than the MP2/6-31(1+3+)G* value. Reducing Khan's calculated VDE by ~0.4 eV brings it well below the experimental value. We conclude that the identity of the $(H_2O)_{24}^-$ isomer or isomers observed in the experiments remains an open question.

IV. Summary

The performance of electronic structure theory for computing vertical electron detachment energies (VDEs) of $(H_2O)_n^-$ has been assessed systematically, as a function of basis set and cluster size. In particular, MP2 and DFT detachment energy predictions have been benchmarked against the experimental results for $n \leq 4$ (where there is agreement regarding the experimentally observed isomers) and against CCSD(T) predictions for $n \leq 6$.

Provided that three shells of diffuse *s* functions are included on the H atoms, both MP2 and CCSD(T) detachment energies are converged to within ~10 meV of their respective complete basis set (CBS) limits, except in cases where the VDE itself is almost zero (or negative), where the basis-set error is ~30−40 meV. Notably, this level of convergence is readily achieved without the use of floating-center basis functions. The atom-centered 6-31(1+3+)G* basis defined herein, consisting of 28 basis functions per water molecule, performs well for VDEs and is not so linearly dependent that one cannot converge self-consistent function (SCF) calculations. Although diffuse Pople-style basis sets have been criticized in the past for being subject to unpredictable fluctuations as the basis size and diffuseness increase,[46] such fluctuations are only an issue when enormous basis sets are used to achieve ~1 meV convergence or better. For the basis sets that are required to achieve the accuracy quoted previously, no such fluctuations are observed. Ironically, the 6-31(1+3+)G* basis that we recommend for VDE calculations is considerably smaller than that required to converge the VDE with respect to molecular geometry optimization, which seems to require a triple-ζ basis to obtain agreement with the experimental values.

Provided that a sufficiently accurate geometry is used, the CBS limit of CCSD(T) reproduces experimental VDEs quantitatively, so we take this as a standard against which lower-level methods may be compared, for a variety of isomers and conformations not necessarily observed in the experiments. We find that second-order Møller−Plesset (MP2) detachment energies are consistently ~30 meV below CCSD(T) values in the same basis set and, significantly, this error is largely independent of the electron binding motif, as well as the magnitude and sign of the VDE. This means that one may utilize small-basis MP2 calculations to estimate VDEs of relatively strong-binding isomers of $(H_2O)_n^-$, in which case the result is probably 30−50 meV too small, but it also implies that such calculations provide useful information, even for isomers that are weakly bound or not bound at all. Granted, if the MP2/6-31(1+3+)G* detachment energy is much less than ~50 meV, one *cannot* use this information to determine whether the isomer in question is actually bound; however, one *can* conclude that it is, at best, bound extremely weakly. For the purpose of screening cluster isomers to assign photoelectron spectra, this may be sufficient.

In regard to density functional theory (DFT), the functionals BLYP, B3LYP, and X3LYP each exhibit significant overbinding at all cluster sizes and for all binding motifs. Notably, this overbinding can easily be obscured by the use of an insufficiently diffuse basis set. The BHLYP functional, in contrast, is considerably more accurate, especially for cluster isomers with small VDEs, where its predictions are only ~30 meV higher than CCSD(T) values. For isomers with large VDEs, BHLYP is up to an order of magnitude less accurate, yet even in these cases, it remains the most accurate density functional for VDE calculations.

Finally, we have performed benchmark VDE calculations on various isomers of $(H_2O)_{20}^-$ and $(H_2O)_{24}^-$. Here, BHLYP and MP2 detachment energies agree to within 400 meV (and are much more similar for certain isomers), which lends credence to our MP2 benchmarks as the most accurate VDEs calculated to date for these systems. Our results cast serious doubt on earlier claims[40−42] to have identified a particular isomer responsible for the photoelectron spectra of each species; the identity of the experimentally observed isomer or isomers of $(H_2O)_{20}^-$ and $(H_2O)_{24}^-$ remains a question for future study.

Acknowledgment. This work was partially supported by the National Science Foundation (NSF), under Grant No. CHE-9981997 (to M.H.-G.) and by an NSF postdoctoral fellowship (to J.M.H.). J.M.H. thanks Art Bragg and Jan Verlet for numerous discussions and for making available their data from ref 14. David J. Anick provided certain optimized geometries for $(H_2O)_{20}$ from ref 89.

References and Notes

(1) Haberland, H.; Ludewigt, C.; Schindler, H.-G.; Worsnop, D. R. *J. Chem. Phys.* **1984**, *81*, 3742.
(2) Haberland, H.; Langosch, H.; Schindler, H.-G.; Worsnop, D. R. *J. Phys. Chem.* **1984**, *88*, 3903.
(3) Coe, J. V.; Lee, G. H.; Eaton, J. G.; Arnold, S. T.; Sarkas, H. W.; Bowen, K. H.; Ludewigt, C.; Haberland, H.; Worsnop, D. R. *J. Chem. Phys.* **1990**, *92*, 3980.
(4) Lee, G. H.; Arnold, S. T.; Eaton, J. G.; Sarkas, H. W.; Bowen, K. H.; Ludewigt, C.; Haberland, H. *Z. Phys. D* **1991**, *20*, 9.
(5) Ayotte, P.; Johnson, M. A. *J. Chem. Phys.* **1997**, *106*, 811.
(6) Ayotte, P.; Bailey, C. G.; Kim, J.; Johnson, M. A. *J. Chem. Phys.* **1998**, *108*, 444.
(7) Ayotte, P.; Weddle, G. H.; Bailey, C. G.; Johnson, M. A.; Vila, F.; Jordan, K. D. *J. Chem. Phys.* **1999**, *110*, 6268.
(8) Kim, J.; Becker, I.; Cheshnovsky, O.; Johnson, M. A. *Chem. Phys. Lett.* **1998**, *297*, 90.
(9) Shin, J.-W.; Hammer, N. I.; Headrick, J. M.; Johnson, M. A. *Chem. Phys. Lett.* **2004**, *399*, 349.
(10) Diken, E. G.; Robertson, W. H.; Johnson, M. A. *J. Phys. Chem. A* **2004**, *108*, 64.
(11) Hammer, N. I.; Shin, J.-W.; Headrick, J. M.; Diken, E. G.; Roscioli, J. R.; Weddle, G. H.; Johnson, M. A. *Science* **2004**, *306*, 675.
(12) Paik, D. H.; Lee, I.-R.; Yang, D.-S.; Baskin, J. S.; Zewail, A. H. *Science* **2004**, *306*, 672.
(13) Bragg, A. E.; Verlet, J. R. R.; Kammrath, A.; Cheshnovsky, O.; Neumark, D. M. *Science* **2004**, *306*, 669.
(14) Verlet, J. R. R.; Bragg, A. E.; Kammrath, A.; Cheshnovsky, O.; Neumark, D. M. *Science* **2005**, *307*, 93.
(15) Mizuno, M.; Tahara, T. *J. Phys. Chem. A* **2001**, *105*, 8823.
(16) Tauber, M. J.; Mathies, R. A. *J. Am. Chem. Soc.* **2003**, *125*, 1394.
(17) Barnett, R. N.; Landman, U.; Cleveland, C. L.; Jortner, J. *J. Chem. Phys.* **1988**, *88*, 4421.
(18) Barnett, R. N.; Landman, U.; Cleveland, C. L.; Jortner, J. *J. Chem. Phys.* **1988**, *88*, 4429.
(19) Barnett, R. N.; Landman, U.; Nitzan, A. *J. Chem. Phys.* **1988**, *89*, 2242.
(20) Coe, J. V. *Int. Rev. Phys. Chem.* **2001**, *20*, 33.

(21) Bartels, D. M. *J. Chem. Phys.* **2001**, *115*, 4404.
(22) Bouteiller, Y.; Desfrançois, C.; Abdoul-Carime, H.; Schermann, J. P. *J. Chem. Phys.* **1996**, *105*, 6420.
(23) Smith, D. M. A.; Smets, J.; Elkadi, Y.; Adamowicz, L. *J. Chem. Phys.* **1997**, *107*, 5788.
(24) Smith, D. M. A.; Smets, J.; Adamowicz, L. *J. Chem. Phys.* **1999**, *110*, 3804.
(25) Lee, S.; Kim, J.; Lee, S. J.; Kim, K. S. *Phys. Rev. Lett.* **1997**, *79*, 2038.
(26) Kim, J.; Park, J. M.; Oh, K. S.; Lee, J. Y.; Lee, S.; Kim, K. S. *J. Chem. Phys.* **1997**, *106*, 10207.
(27) Kim, K. S.; Lee, S.; Kim, J.; Lee, J. Y. *J. Am. Chem. Soc.* **1997**, *119*, 9329.
(28) Kim, J.; Suh, S. B.; Kim, K. S. *J. Chem. Phys.* **1999**, *111*, 10077.
(29) Kim, J.; Lee, J. Y.; Oh, K. S.; Park, J. M.; Lee, S.; Kim, K. S. *Phys. Rev. A* **1999**, *59*, R930.
(30) Suh, S. B.; Lee, H. M.; Kim, J.; Lee, J. Y.; Kim, K. S. *J. Chem. Phys.* **2000**, *113*, 5273.
(31) Lee, H. M.; Lee, S.; Kim, K. S. *J. Chem. Phys.* **2003**, *119*, 187.
(32) Lee, H. M.; Suh, S. B.; Tarakeshwar, P.; Kim, K. S. *J. Chem. Phys.* **2005**, *122*, 044309.
(33) Tsurusawa, T.; Iwata, S. *Chem. Phys. Lett.* **1998**, *287*, 553.
(34) Weigend, F.; Ahlrichs, R. *Phys. Chem. Chem. Phys.* **1999**, *1*, 4537.
(35) Chen, H.-Y.; Sheu, W.-S. *J. Chem. Phys.* **1999**, *110*, 9032.
(36) Alfonso, D. R.; Jordan, K. D. *J. Chem. Phys.* **2002**, *116*, 3612.
(37) Wang, F.; Jordan, K. D. *J. Chem. Phys.* **2002**, *116*, 6973.
(38) Novakovskaya, Y. V.; Stepanov, N. F. *Int. J. Quantum Chem.* **2004**, *88*, 496.
(39) Novakovskaya, Y. V.; Stepanov, N. F. *Struct. Chem.* **2004**, *15*, 65.
(40) Khan, A. *J. Chem. Phys.* **2003**, *118*, 1684.
(41) Khan, A. *J. Chem. Phys.* **2004**, *121*, 280.
(42) Khan, A. *Chem. Phys. Lett.* **2005**, *401*, 85.
(43) Tachikawa, H. *Chem. Phys. Lett.* **2003**, *370*, 188.
(44) Sobolewski, A. L.; Domcke, W. *Chem. Phys.* **2003**, *294*, 73.
(45) Gutowski, M.; Jordan, K. D.; Skurski, P. *J. Phys. Chem. A* **1998**, *102*, 2624.
(46) Skurski, P.; Gutowski, M.; Simons, J. *Int. J. Quantum Chem.* **2000**, *80*, 1024.
(47) Hehre, W. J.; Radom, L.; v. R. Schleyer, P.; Pople, J. A. *Ab Initio Molecular Orbital Theory*; Wiley: New York, 1986.
(48) Becke, A. D. *Phys. Rev. A* **1988**, *38*, 3098.
(49) Lee, C.; Yang, W.; Parr, R. G. *Phys. Rev. B* **1988**, *37*, 785.
(50) Becke, A. D. *J. Chem. Phys.* **1993**, *98*, 5648.
(51) Stephens, P. J.; Devlin, J. F.; Chabalowski, C. F.; Frisch, M. J. *J. Phys. Chem.* **1994**, *98*, 11623.
(52) Becke, A. D. *J. Chem. Phys.* **1993**, *98*, 1372.
(53) We use BHLYP as defined by King et al., $E_{XC}^{BHLYP} = (1/2)E_X^{Slater} + (1/2)E_X^{HF} + E_C^{LYP}$ (see refs 79−81). This functional differs from that proposed by Becke in ref 52.
(54) Bartlett, R. J. In *Modern Electronic Structure Theory, Part II*; Yarkony, D. R., Ed.; World Scientific: Rivers Edge, NJ, 1995; p 1047.
(55) Xu, X.; Goddard, W. A., III. *Proc. Natl. Acad. Sci. U.S.A.* **2004**, *101*, 2673.
(56) Su, J. T.; Xu, X.; Goddard, W. A., III. *J. Phys. Chem. A* **2004**, *108*, 10518.
(57) Xu, X.; Zhang, Q.; Muller, R. P.; Goddard, W. A., III. *J. Chem. Phys.* **2005**, *122*, 014105.
(58) Kong, J.; White, C. A.; Krylov, A. I.; Sherrill, C. D.; Adamson, R. D.; Furlani, T. R.; Lee, M. S.; Lee, A. M.; Gwaltney, S. R.; Adams, T. R.; Ochsenfeld, C.; Gilbert, A. T. B.; Kedziora, G. S.; Rassolov, V. A.; Maurice, D. R.; Nair, N.; Shao, Y.; Besley, N. A.; Maslen, P. E.; Dombroski, J. P.; Daschel, H.; Zhang, W.; Korambath, P. P.; Baker, J.; Byrd, E. F. C.; Van Voorhis, T.; Oumi, M.; Hirata, S.; Hsu, C.; Ishikawa, N.; Florian, J.; Warshel, A.; Johnson, B. G.; Gill, P. M. W.; Head-Gordon, M.; Pople, J. A. *J. Comput. Chem.* **2000**, *21*, 1532.
(59) Schaftenaar, G.; Noordik, J. H. *J. Comput.-Aided Mol. Design* **2000**, *14*, 123.
(60) Humphrey, W.; Dalke, A.; Schulten, K. *J. Mol. Graphics* **1996**, *14*, 33.
(61) Dolgounitcheva, O.; Zakrzewski, V. G.; Ortiz, J. V. *Chem. Phys. Lett.* **1999**, *307*, 220.
(62) Jensen, F. *J. Chem. Phys.* **2002**, *117*, 9234.
(63) Van Voorhis, T.; Head-Gordon, M. *Mol. Phys.* **2002**, *100*, 1713.
(64) Gill, P. M. W.; Johnson, B. G.; Pople, J. A. *Chem. Phys. Lett.* **1993**, *209*, 506.
(65) Note that the radial quadrature scheme used in DFT calculations (see ref 66) maps the interval [0, 1] onto [0, ∞], so adding more radial grid points extends the grid to larger radial values. Experimenting with a denser grid thus probes whether there are sufficient grid points in regions of diffuse electron density.
(66) Murray, C. W.; Handy, N. C.; Laming, G. J. *Mol. Phys.* **1993**, *78*, 997.
(67) Tozer, D. J.; Handy, N. C.; Amos, R. D.; Pople, J. A.; Nobes, R. H.; Xie, Y.; Schaefer, H. F., III. *Mol. Phys.* **1993**, *79*, 777.
(68) Byrd, E. F. C.; Sherrill, C. D.; Head-Gordon, M. *J. Phys. Chem. A* **2001**, *105*, 9736.
(69) Handy, N. C.; Knowles, P. J.; Somasundrum, K. *Theor. Chim. Acta* **1985**, *68*, 87.
(70) Nobes, R. H.; Pople, J. A.; Radom, L.; Handy, N. C.; Knowles, P. J. *Chem. Phys. Lett.* **1987**, *138*, 481.
(71) Gill, P. M. W.; Radom, L. *Chem. Phys. Lett.* **1986**, *132*, 16.
(72) Gill, P. M. W.; Pople, J. A.; Radom, L.; Nobes, R. H. *J. Chem. Phys.* **1988**, *89*, 7307.
(73) Lepetit, M. B.; Pélissier, M.; Malrieu, J. P. *J. Chem. Phys.* **1988**, *89*, 998.
(74) Gutowski, M.; Skurski, P.; Boldyrev, A. I.; Simons, J.; Jordan, K. D. *Phys. Rev. A* **1996**, *54*, 1906.
(75) Gutowski, M.; Skurski, P. *J. Phys. Chem. B* **1997**, *101*, 9143.
(76) Skurski, P.; Gutowksi, M. *J. Chem. Phys.* **1998**, *108*, 6303.
(77) Skurski, P.; Gutowski, M.; Simons, J. *J. Chem. Phys.* **1997**, *110*, 274.
(78) Rak, J.; Skurski, P.; Gutowski, M. *J. Chem. Phys.* **2001**, *114*, 10673.
(79) King, R. A.; Galbraith, J. M.; Schaefer, H. F., III. *J. Phys. Chem. A* **1996**, *100*, 6061.
(80) King, R. A.; Mastryukov, V. S.; Schaefer, H. F., III. *J. Chem. Phys.* **1996**, *105*, 6880.
(81) King, R. A.; Pettigrew, N. D.; Schaefer, H. F., III. *J. Chem. Phys.* **1997**, *107*, 8536.
(82) Rienstra-Kiracofe, J. C.; Tschumper, G. S.; Schaefer, H. F., III; Sreela, N.; Ellison, G. B. *Chem. Rev.* **2002**, *102*, 231.
(83) Weimer, M.; Della Sala, F.; Görling, A. *Chem. Phys. Lett.* **2003**, *372*, 538.
(84) Hendricks, J. H.; de Clercq, H. L.; Lyapustina, S. A.; Fancher, C. A.; Lippa, T. P.; Collins, J. M.; Arnold, S. T.; Lee, G. H.; Bowen, K. H. In *Structures and Dynamics of Clusters*; Kondow, T., Ed.; Proceedings of the Yamada Conference XLIII; Universal Academy: Tokyo, 1995.
(85) Bauschlicher, C. W., Jr.; Langhoff, S. R.; Partridge, H.; Taylor, P. R. *J. Chem. Phys.* **1986**, *85*, 3407.
(86) Feller, D.; Davidson, E. R. *J. Chem. Phys.* **1989**, *90*, 1024.
(87) Our $(H_2O)_4^-$ isomers A, B, and C correspond, respectively, to what Lee et al. call 4Rf(4Rdd2), 4Rf′(4Rdd1), and 4R (see ref 31).
(88) Jeffrey, G. A. In *Inclusion Compounds*; Atwood, J. L., Davies, J. E. D., MacNichol, D. D., Eds.; Academic Press: London, 1984; Vol. 1, p 135.
(89) Anick, D. J. *J. Chem. Phys.* **2003**, *119*, 12442.
(90) Fanourgakis, G. S.; Aprà, E.; Xantheas, S. S. *J. Chem. Phys.* **2004**, *121*, 2655.
(91) Khan, A. *Chem. Phys. Lett.* **1994**, *217*, 443.
(92) Khan, A. *Chem. Phys. Lett.* **1996**, *253*, 299.
(93) Khan, A. *J. Chem. Phys.* **1999**, *110*, 11884.
(94) Khan, A. *J. Mol. Struct. (THEOCHEM)* **2003**, *664*, 237.
(95) Kirov, M. V. *J. Struct. Chem.* **2002**, *43*, 790.
(96) Chihaia, V.; Adams, S.; Kuhs, W. F. *Chem. Phys.* **2004**, *297*, 271.
(97) Kabrede, H.; Hentschke, R. *J. Phys. Chem. B* **2003**, *107*, 3914.